Analysis of multiple cosmogenic nuclides constrains Laurentide Ice Sheet history and process on Mt. Mansfield, Vermont's highest peak

For submission to Quaternary Science Reviews

Lee B. Corbett a*
Paul R. Bierman a
Stephen F. Wright a
Jeremy D. Shakun b
P. Thompson Davis c
Brent M. Goehring d
Christopher T. Halsted b,a
Alexandria J. Koester b,f
Marc W. Caffee e,f
Susan R. Zimmerman g

^{*}Corresponding Author: Ashley.Corbett@uvm.edu, (802) 380-2344

^a Department of Geology, University of Vermont, Burlington, VT, USA

^b Department of Earth and Environmental Sciences, Boston College, Boston, MA, USA

^c Department of Natural and Applied Science, Bentley University, Waltham, MA, USA

^d Department of Earth and Environmental Sciences, Tulane University, New Orleans, LA, USA

^e Department of Physics and Astronomy, Purdue University, West Lafayette, IN, USA

f Department of Earth, Atmospheric, and Planetary Sciences, Purdue University, West Lafayette, IN, USA

⁹ Center for Accelerator Mass Spectrometry, Lawrence Livermore National Laboratory, Livermore, CA, USA

Abstract

45

46

47

48

49

50 51

52

53

54 55

56

57 58

59

60

61

62

63

64 65

66

Constraining glacial history and process on Mt Mansfield, the highest peak in Vermont (1339 m a.s.l.), provides insight into how the Laurentide Ice Sheet shaped the underlying landscape, when latest Pleistocene ice retreated, and how upland and lowland glacial histories relate. Here , we quantify in situ cosmogenic ¹⁰Be in 20 bedrock and boulder surfaces, as well as in situ cosmogenic ¹⁴C in three of those surfaces, to assess subglacial erosion and exposure history. Isotopic concentrations indicate that Mt. Mansfield's lower elevations (~400-1200 m a.s.l.) were deeply eroded by at least several meters during the last glaciation and then deglaciated rapidly; 10 Be ages across this elevation span are indistinguishable and average 13.9 \pm 0.6 ka (n = 15), suggesting that 800 m of ice thinning occurred within at most about a millennium. Conversely, the higher elevations (>1200 m a.s.l.) preserve a more complex geomorphic history. Mt. Mansfield's summit surfaces contain ¹⁰Be from previous periods of exposure, indicating that the mountaintop landscapes were likely preserved beneath cold-based, weakly-erosive glacial ice. Exposure ages from the shorter-lived isotope, ¹⁴C, are younger (9.7 and 11.7 ka), suggesting that Mt. Mansfield's summit was covered until the early Holocene, perhaps by snowfields, ice carapaces, and/or till. Our findings, in context of previous work, suggest that thinning Laurentide ice flowed through the valleys for at most hundreds of years following deglaciation of the uplands, but that the summit remained shielded by ice or sediment for millennia after the valleys became ice-free.

Keywords: Pleistocene; Last Glacial Maximum; glaciation; North America; geochronology; cosmogenic isotopes; erosion

1. Introduction

68 pro
69 How
70 nor
71 of F
72 var
73 and
74 The
75

The retreat of the Laurentide Ice Sheet (LIS) after the Last Glacial Maximum (LGM) provides important context for understanding ice dynamics in a warming world (Long, 2009). However, the bulk of the evidence constraining LIS retreat chronology and process in the northeastern United States is biased toward low-elevation depositional settings (see the review of Ridge et al. (1999)). Such evidence includes a high-resolution chronology developed from varves in proglacial lakes (Ridge et al., 2012), basal radiocarbon ages of sediment cores (Davis and Jacobson, 1985), radiocarbon ages of depositional features such as glaciomarine deltas (
Thompson et al., 1989), and cosmogenic nuclide exposure ages of major moraine segments
ADDIN EN.CITE (Balco et al., 2009; Balco and Schaefer, 2006; Balco et al., 2002; Bromley et al., 2015; Corbett et al., 2017; Davis et al., 2015; Hall et al., 2017; Koester et al., 2017).

Higher-elevation areas hold unique and important additional information regarding ice sheet behavior and deglaciation chronology. For example, cosmogenic nuclide data suggest that weakly-erosive ice covered at least some of the highest peaks in the northeastern United States (Bierman et al., 2015) and much of the uplands in eastern Canada ADDIN EN.CITE (Briner et al., 2014; Briner et al., 2006; Corbett et al., 2016a; Margreth et al., 2016). Vertical profiles of mountain-side cosmogenic nuclide exposure ages can constrain the timing and rate of ice thinning ADDIN EN.CITE (Goehring et al., 2008; Johnson et al., 2014; Koester et al., 2017; Stone et al., 2003; Winsor et al., 2015) and/or the juxtaposition of altitude-dependent weathering regimes (Stone et al., 1998; Sugden et al., 2005). Uplands in the northeastern United States thus represent an understudied but useful landscape for assessing glacial history and process (Miller et al., 2006).

Mt. Mansfield, Vermont's highest peak (1339 m a.s.l., Fig. 1), provides a high-elevation landscape for assessing ice erosivity, the timing of ice sheet thinning, and the rate of ice margin retreat in western New England. Mt. Mansfield is bordered to the west by the Champlain valley (occupied by glacial Lake Vermont during deglaciation) and to the east by the Connecticut River valley (occupied by glacial Lake Hitchcock during deglaciation), both of which have been studied extensively (see reviews in Rayburn et al. (2007) and Ridge et al. (2012)). The close juxtaposition of these landscape features allows us to study the relationship between upland and lowland glacial dynamics. Here, we report field observations as well as measured concentrations of *in situ* cosmogenic ¹⁰Be and ¹⁴C from Mt. Mansfield bedrock and boulder surfaces to assess how Laurentide ice shaped the landscape, when and how rapidly northern Vermont was deglaciated, and how the upland history fits with the better-studied lowland history of regional deglaciation.

2. Study Area and Previous Work

2.1. Mt. Mansfield

Mt. Mansfield (Figs. 1 and 2, elevation 1339 m a.s.l.) is Vermont's highest peak, located in the north-central part of the state, along the spine of the Green Mountains. Mt. Mansfield is ~35 km east of the Champlain valley and ~100 km west of the Connecticut River valley. The study area is underlain by rocks of the Underhill Formation, composed of Neoproterozoic and Cambrian metamorphic rocks (Ratcliffe et al., 2011) that contain sufficient quartz for analysis of *in situ* cosmogenic ¹⁰Be and ¹⁴C. The landscape in the study area is subalpine and alpine, dominated by conifers, with the highest elevations just above tree line. Following deglaciation, the summit has served as a high-elevation refuge for plants that still persist in the warmer

modern climate and grow in alpine soils (Munroe et al., 2007).

Field observation reveals evidence of prior glaciation. Striations are visible on many bedrock surfaces and show multiple directions of ice flow including NW-SE along most of Mt. Mansfield's summit ridge, N-S in some lower elevation areas, and W-E in the valley south of Mt. Mansfield (Fig. 2). At lower elevations, bedrock outcrops are rounded and sculpted (Fig. 3a); however, at higher elevations, outcrops sometimes exhibit frost shattering (Fig. 3b). In areas where the mountain slopes are mantled by thick accumulations of till, such till frequently forms distinct step-like moraines (Fig. 2). Recent mapping has confirmed that these features are not cored by bedrock and do not show signs of mass movement (Wright, 2018). Continuous parallel flights of moraines are clearly visible on the LiDAR imagery where they gently slope into tributary valleys, with spacing between adjacent moraines typically ranging between 20 and 75 m (Fig. 2).

2.2. Previous Work: Mt. Mansfield Area

Mt. Mansfield has long been the subject of geologic inquiry, beginning with the work of Hitchcock et al. (1861). The occurrence of glacial striations (Hungerford, 1868) and erratic boulders on the summit ridge (Christman, 1959; Hitchcock et al., 1861) provided the initial evidence that even the highest elevations had been covered by a large, continental-scale ice sheet. While some researchers postulated that large sediment ridges on Mt. Mansfield's east side were end moraines formed by an episode of cirque glaciation that post-dated regional glaciation (Wagner, 1970), others argued that steep valleys on the mountainside were formed prior to the LGM ADDIN EN.CITE (Davis, 1999; Loso et al., 1998; Waitt and Davis, 1988) and

that the ridges originally interpreted as end moraines of cirque glaciers near Mt. Mansfield were instead eskers formed beneath the retreating ice sheet (Wright et al., 1997).

133

134

135

136

137

138

139

140

141

142

143

144

145

146

147

148

149

150

151

152

153

154

The timing of deglaciation of the summit region is unknown. The only nearby age data come from Sterling Pond ~4 km northeast of the summit and ~400 m lower in elevation (Fig. 1). Here, an organic radiocarbon measurement (hereafter organic ¹⁴C, to differentiate from *in situ* 14 C) from bulk sediment at the base of a core yielded an age of 12760 \pm 70 14 C yr BP (Lin, 1996), or 15100-15300 cal yr BP (1σ age range, Table 1, all organic 14 C ages have been recalibrated using Calib version 7.1 (Stuiver et al., 2015) and the IntCal13 calibration curve (Reimer et al., 2013)). This age, if correct, is a minimum limit for the timing of summit deglaciation because it is considerably lower in elevation (919 m) than the summit (1339 m) and would have been buried by ice after Mt. Mansfield's summit became exposed as the ice thinned. However, bulk lake sediment organic 14C ages may be inaccurate. On one hand, there is an unknown lag time needed for vegetation to become established and organic material enter the lake basin (Davis and Davis, 1980); on the other hand, bulk lake sediment ages are often too old because they contain recycled carbon (Davis et al., 1995) or are subject to hard water effects (Shotton, 1972). Several studies in Vermont have shown organic macrofossil ages to be hundreds of years younger than bulk sediment ages ADDIN EN.CITE (Brown, 1999; Noren, 2002; Parris, 2003), likely because of carbon recycling.

2.3. Previous Work: North-Central Vermont and Post-Glacial Lakes

Chronologic data from the glacial lake valleys to the west and east of Mt. Mansfield (Ridge, 2004) provide context for the deglaciation of the study area. Because lakes in these valleys did not form until the valleys became ice-free, ages from the glacial lake sediments provide minimum limits for the deglaciation of Mt. Mansfield. To the west, the Champlain valley (Fig. 1) contained glacial Lake Vermont ADDIN EN.CITE (Chapman, 1937; Rayburn et al., 2005; Ridge, 2004). Macrofossils from glacial Lake Vermont sediments have organic ¹⁴C ages of 10900 \pm 75 14 C yr BP (Rayburn et al., 2007) and 11360 \pm 115 14 C yr BP (Cadwell et al., 1991; Rayburn et al., 2007), yielding calibrated ages of 12710-12830 and 13100-13300 cal yr BP respectively (1 σ age ranges, Table 1). To the east, varve chronologies from glacial Lake Hitchcock sediments in the Connecticut River valley (Fig. 1) place the retreating LIS margin at the same latitude as Mt. Mansfield after 13900 cal yr BP (Ridge et al., 2012), following abandonment of the Littleton-Bethlehem moraine in northern New Hampshire (Thompson et al., 2017). Along the eastern border of the Green Mountains, varves from glacial Lake Winooski (Larsen, 1972, 1987), when correlated with the North American Varve Chronology (Ridge et al., 2012), indicate that the lake existed from ~14100 to 13820 cal yr BP (Larsen et al., 2003; Wright, 2018). The formation of Lake Winooski at ~14100 cal yr BP represents the most geographically proximal minimum limit for the deglaciation of Mt. Mansfield as constrained by glacial lakes.

155

156

157

158

159

160

161

162

163

164

165

166

167

168

169

170

171

172

173

174

175

176

In addition to information from glacial lakes, basal organic ¹⁴C ages from sediment cores of small, upland lakes and ponds in the northern half of Vermont, northeastern New York, and northern New Hampshire (Table 1, Fig. 1) provide additional constraints for the timing of deglaciation (Ridge et al., 1999). However, due to the uncertainties discussed above, particularly the recycling of old carbon in bulk sediments (Davis et al., 1995) and the unknown

lag time between deglaciation and organic sedimentation (Davis and Davis, 1980), basal sediment core ages vary widely. Ages from material at the bottoms of lake sediment cores range from 13000 to 9155 ¹⁴C yr BP ADDIN EN.CITE (Bierman et al., 1997; Davis et al., 1980; Lin, 1996; McDowell et al., 1971; Munroe, 2012; Noren et al., 2002; Parris et al., 2010; Rogers et al., 2009; Spear, 1989; Spear et al., 1994; Sperling et al., 1989; Thompson et al., 1996; Whitehead and Jackson, 1990), yielding calibrated ages of 15490-10350 yr BP (Table 1, Fig. 1). Compilations of radiocarbon ages from the northeastern United States, including those from New York, Vermont, New Hampshire, Massachusetts, and Maine, show a similarly wide spread of ages (Davis and Jacobson, 1985; Gaudreau and Webb, 1985).

3. Background: in situ Cosmogenic ¹⁰Be and ¹⁴C

In situ produced cosmogenic nuclides, primarily ¹⁰Be in quartz, have been used since the 1980s to determine the timing and rates of deglaciation ADDIN EN.CITE (Balco, 2011; Bierman , 1994; Fabel and Harbor, 1999; Gosse et al., 1995; Nishiizumi et al., 1989; Phillips et al., 1990). These nuclides accumulate at known rates in rock surfaces exposed to cosmic rays (Lal, 1988); determining the concentration of the nuclide of interest in rock surfaces quantifies the duration of time that has elapsed since deglaciation ADDIN EN.CITE (Gosse and Phillips, 2001; Nishiizumi et al., 1993). However, interpreting a cosmogenic nuclide measurement as an exposure age relies on several assumptions: (1) that nuclides from previous periods of exposure were removed by erosion of at least several meters during the most recent glaciation (Briner et al., 2016), (2) that surfaces were not shielded by snow or sediment following deglaciation (Heyman et al., 2016; Schildgen et al., 2005), and (3) that surfaces have not been eroded

following deglaciation (Zimmerman et al., 1994). If these assumptions are not met, then calculated ages over-estimate (in the case of inherited nuclides) or under-estimate (in the case of shielding and/or erosion) the timing of actual exposure.

We employ two different *in situ* cosmogenic nuclides produced in quartz that have different half-lives: ¹⁰Be (1.38 Ma) and ¹⁴C (5.73 ka). Measuring the shorter-lived nuclide is useful for isolating recent exposure (i.e. exposure since the last deglaciation) because most *in situ* ¹⁴C produced before the LGM has decayed away due to the 5.73 ka half-life ADDIN EN. CITE (Briner et al., 2014; Goehring et al., 2011; Miller et al., 2006). *In situ* ¹⁴C has been used only sparsely in the northeastern United States; latest Pleistocene ¹⁴C ages on the summits of Katahdin and Mt. Washington, the highest points in Maine and New Hampshire respectively, demonstrate that those summits were covered by LGM ice even though the associated ¹⁰Be exposure ages are much older due to the presence of inherited nuclides (Bierman et al., 2015).

Paired ¹⁴C/¹⁰Be data are typically plotted on a two-isotope diagram, with ¹⁴C/¹⁰Be on the vertical axis and ¹⁰Be concentration on the horizontal axis (Goehring et al., 2011). Samples can plot along a constant exposure pathway, in an envelope consistent with constant exposure and erosion, or below the exposure/erosion envelope in a zone indicative of at least one period of burial following initial exposure. Although inferences from ¹⁴C/¹⁰Be are non-unique, using the two nuclides in tandem can provide information about complex scenarios involving exposure, erosion, and burial. This is similar to the ²⁶Al/¹⁰Be system (Granger and Muzikar, 2001), although the difference between half-lives for ¹⁴C/¹⁰Be is much greater than for ²⁶Al/¹⁰Be, yielding insight about processes over a more recent timescale (tens of ka).

4. Methods

4.1. Sample Collection, Preparation, and Analysis

We collected samples during 2015-2017 from 20 bedrock and boulder surfaces using a hammer and chisel (Table 2, Figs. 3 and 4). Samples span from 411 to 1305 m a.s.l. and are from Mt. Mansfield's lowlands, ridges, and summit. We avoided sampling surfaces that exhibited evidence of significant subaerial erosion and boulders that may have rolled. At each sample site , we used high-precision GPS to record latitude, longitude, and elevation; we measured thickness and shielding, and made observations about sample surface characteristics. We isolated quartz for *in situ* ¹⁰Be and ¹⁴C analyses at University of Vermont following the methods of Kohl and Nishiizumi (1992).

We extracted beryllium (n = 20) in the University of Vermont Cosmogenic Nuclide Laboratory with methods described in Corbett et al. (2016b) and using ~20 g of quartz per sample. We spiked each sample with ~250 μ g Be using an in-house-made beryl carrier (Table 3). Samples were prepared in batches of 12, including ten unknowns, one blank, and one quality control standard (CRONUS N, Jull et al. (2015)), along with other late-Pleistocene age samples from the northeastern United States and southeastern Canada. Accelerator Mass Spectrometry (AMS) analysis of 10 Be/ 9 Be occurred at Livermore National Laboratory (LLNL) and Purdue Rare Isotope Measurement (PRIME) Laboratory (Table 3), with ratios normalized to standard 07KNSTD3110, which has an assumed ratio of 2.850 x 10^{-12} (Nishiizumi et al., 2007). We corrected samples for backgrounds using the average and standard deviation of blanks from the same AMS, correcting LLNL samples to the LLNL blanks (n = 4, 1.08 \pm 0.46 x 10^{-15}) and PRIME samples to the PRIME blanks (n = 4, 0.74 \pm 0.20 x 10^{-15}), and propagating uncertainties in quadrature (Table 3). Background-corrected sample ratios range from 0.92 to 3.90 x 10^{-13} ;

analytic uncertainties (including the propagated blank uncertainty) are 2.5 \pm 0.8 % (average, 1SD).

Extraction of carbon for *in situ* 14 C analyses (n = 3) took place at Tulane University (Goehring et al., Accepted) using ~3.0 g of quartz per sample fused via LiBO₂ (Table 4). AMS analysis of 14 C/ 13 C ratios took place at the National Ocean Sciences Accelerator Mass Spectrometry facility, with sample ratios normalized to primary standard Ox-II with an assumed ratio of 1.4575 x $^{10^{-10}}$. We corrected samples for backgrounds using the average and standard deviation of the long-term process blank for the Tulane system (1.019 \pm 0.079 x $^{10^5}$ atoms; Goehring et al. (Accepted)). Stable 13 C/ 12 C ratios were measured at the UC Davis Stable Isotope Facility. 14 C/C sample ratios range from 1.41 to 1.58 x $^{10^{-13}}$; analytic uncertainties (including the propagated blank uncertainty) are 1.7% for the three samples.

4.2. Exposure Age Calculations

We calculated ¹⁰Be and ¹⁴C exposure ages (Table 5) with Version 3 of the online exposure age calculator formerly known as CRONUS Earth (Balco et al., 2008) and the regionally -calibrated northeastern North American production rate dataset (Balco et al., 2009). We implement "LSDn" scaling because it uses nuclide-specific equations that reflect the differences between ¹⁰Be and ¹⁴C production ADDIN EN.CITE (Borchers et al., 2016; Lifton, 2016; Lifton et al., 2014). The calculated ages assume no nuclides inherited from previous exposure and no post-exposure erosion or shielding.

Because previous cosmogenic nuclide studies in the northeastern United States have been published using other production rates and scaling schemes, we recalculated relevant

cosmogenic ages from the region using the regionally-calibrated northeastern North American production rate dataset (Balco et al., 2009) and the "LSDn" scaling. The regional ages we cite throughout the Discussion are these recalculated ages so that they are directly comparable to the Mt. Mansfield ages.

5. Results

Background-corrected sample 10 Be concentrations are 0.766 - 2.88 x 10^5 atoms g^{-1} (Table 3), yielding exposure ages of 12.9 ± 0.4 to 22.9 ± 0.5 ka (1σ internal uncertainties, Table 5, Figs. 4 and 5). In the one instance where we sampled bedrock (MM-02, 14.8 ± 0.3 ka) and boulder (MM-01, 14.5 ± 0.3 ka) surfaces in close proximity (at 1170 m a.s.l.), the two ages agree within 1σ internal uncertainties (Fig. 4). In general, exposure ages increase with elevation (Fig. 5); samples below ~1200 m a.s.l. form an overlapping population of ages (average 13.9 ± 0.6 ka, n = 15, 1SD) and samples above ~1200 m a.s.l. are older (15.0-22.9 ka).

Background-corrected sample 14 C concentrations are 2.16 - 2.41 x 105 atoms $^{-1}$ (Table 4), yielding exposure ages of 9.7 - 15.6 ka (Table 5, Figs. 4 and 5). For the lower-elevation boulder sample (MM-03, 1176 m a.s.l.), the 10 Be (13.7 \pm 1.2 ka) and *in situ* 14 C (15.6 \pm 2.5 ka) ages agree within 1 O external uncertainties (Fig. 4; we use external uncertainties here because of the differing production rate calibrations and scaling). Conversely, closer to the summit, in samples of bedrock, there are significant mismatches between the exposure ages generated with the two nuclides (MM-08, 10 Be $^{17.4}$ \pm 1.5 ka, 14 C $^{11.7}$ \pm 1.4 ka; and MM-09, 10 Be $^{22.9}$ \pm 2.0 ka, 14 C 9.7 \pm 1.0 ka). The 14 C/ 10 Be ratios (Fig. 6) suggest that one sample (MM-08) is consistent with constant exposure with erosion; the other samples fall just above (MM-03) or just below (

MM-09) the exposure/erosion envelope based on 1σ uncertainties, but overlap within 2σ .

6. Discussion

6.1. The Lower Elevations: Efficient Subglacial Erosion Followed by Rapid Thinning

Mt Mansfield's lower elevations (~400-1200 m a.s.l.) were deeply eroded by the LIS, yielding fresh, glacially sculpted landscapes following deglaciation. This erosion is evidenced by the agreement between bedrock and boulder exposure ages and is also suggested by the agreement between exposure ages generated with different nuclides on the same sample surface (Figs. 4 and 5). The agreement between 10 Be and 14 C ages indicates that at least several meters of rock were removed from exposed surfaces during the last glaciation, leaving behind minimal inherited 10 Be (the longer-lived nuclide) from pre-LGM exposure. The exposure ages at lower elevations therefore record the timing of exposure and yield an estimate of deglaciation at ~13.9 \pm 0.6 ka (10 Be, n = 15, average, 1SD).

At these lower elevations, deglaciation occurred rapidly, exposing all of the sample surfaces between about 400 and 1200 m a.s.l. simultaneously within the resolution of the in situ 10 Be chronometer. Similarly rapid thinning in Maine (Koester et al., 2017), New Hampshire (Davis et al., 2017), and Norway (Goehring et al., 2008), as well as rapid retreat through fjords in Greenland (Corbett et al., 2013) and on Baffin Island (Briner et al., 2009), has been inferred on the basis of indistinguishable 10 Be age populations. In Maine (Koester et al., 2017), the episode of rapid thinning that took place at 15.3 ± 0.5 ka (n = 16, average, 1SD, recalculated as described above), is older than the thinning episode that exposed Mt. Mansfield; a two-tailed, unequal variance t-test demonstrates that the age populations are statistically separable (p < 0.

01). The exposure of Mansfield's middle and lower elevations occurred likely within several centuries and probably no more than a millennium (see the statistical simulations described in Koester et al. (2017)), suggesting rapid surface lowering of the LIS margin in northern New England. The period of rapid thinning that occurred on Mt. Mansfield at 13.9 ± 0.6 ka slightly post-dates the abrupt onset of warm temperatures recorded in the GISP2 ice core during the Bølling-Allerød warm period commencing ~14.6 ka (Buizert et al., 2014; Clark et al., 2001), as simulated in the Mt. Mansfield region with paleoclimate models (Fig. 7).

6.2. The Higher Elevations: Complex Geomorphic Processes

Data from Mt. Mansfield's uplands demonstrate that the geomorphic history at high elevations is more complicated than at lower elevations. The presence of two young in situ ¹⁴C ages (11.7 and 9.7 ka, both from surfaces with older ¹⁰Be ages) suggests that Mt. Mansfield's summit was shielded by ice, snow, and/or till for longer than lower elevation areas. Both of these samples have ¹⁴C/¹⁰Be ratios that are indistinguishable from constant exposure within 2σ , suggesting that they have experienced no or minimal burial since initial exposure at the beginning of the Holocene, and hence that all or most of their ¹⁴C has accumulated in a single period. These young exposure ages (as compared to the ~13.9 ka exposure ages at lower elevations) imply that bedrock surfaces at the highest elevations were isolated from nuclide production until several ka after the LIS margin had retreated from the region. The close agreement between ¹⁰Be and in situ ¹⁴C exposure ages at a lower elevation site (sample MM-03) suggests that prolonged shielding was restricted to the summit region.

Post deglaciation shielding of samples collected from Mt. Mansfield's summit could be the result of numerous geomorphic processes, including cover by thick snow, stagnant ice, and/or till. In the case of ice or snow, small snowfields or carapaces could have remained behind following rapid LIS thinning (although this is unlikely given how rapidly the ice sheet was losing mass at that time, Lambeck et al. (2014)) or could have regenerated. In the case of till, sediment cover could have existed for millennia following deglaciation, eventually eroding away to expose bedrock surfaces. Although there is abundant till on Mt. Mansfield's flanks, there is virtually no till on the summit today, so it was either never there or has been completely removed. Regardless of the shielding mechanism, the summit surfaces were ultimately exposed in the early Holocene, perhaps driven by regional warming (Fig. 7) also observed in paleoenvironmental proxies in nearby Sterling Pond (Lin, 1996), Nulhegan Pond, and Beecher Pond (Fig. 1; Munroe (2012)). If exposure of the summit occurred gradually, through slow melting of ice/snow or progressive stripping of till, then the bedrock surfaces we analyzed would have received a portion of their nuclide concentrations through thin cover and partial shielding; in that case, the in situ 14C ages represent maximum limits for the time at which bedrock surfaces became bare.

330

331

332

333

334

335

336

337

338

339

340

341

342

343

344

345

346

347

348

349

350

351

Assuming the *in situ* ¹⁴C ages record the time of exposure of Mt. Mansfield's summit, then the ¹⁰Be concentrations must contain a large inventory of nuclides inherited from pre-LGM exposure (because ¹⁰Be is the longer-lived nuclide and decay during LGM burial was negligible). In that case, assuming an exposure time of 10.7 ka (the average of the two summit *in situ* ¹⁴C ages), the high-elevation surfaces are carrying an excess of ~4-12 ka of ¹⁰Be, or ~30-50% of their total nuclide concentrations. These old ¹⁰Be exposure ages do not represent early thinning of

the LIS and exposure of Mt. Mansfield's summit at ~23 ka (the exposure ¹⁰Be age of bedrock surface MM-09) because the young *in situ* ¹⁴C ages preclude this possibility and because the ice margin was at its terminal position several hundred km south of the study area at that time (Balco et al., 2002; Corbett et al., 2017). Further, the heterogeneity of the high-elevation ¹⁰Be exposure ages is more indicative of variable sub-glacial erosion, which often creates a scattered population of ages (Briner et al., 2005), instead of early exposure, which would result in a single population of older exposure ages.

352

353

354

355

356

357

358

359

360

361

362

363

364

365

366

367

368

369

370

371

372

373

Significant inherited ¹⁰Be from pre-LGM exposure could persist in Mt. Mansfield's high elevations due to cold-based ice with limited erosive power (Kleman and Borgstrom, 1994) covering Vermont's highest topography and/or because the duration of ice flow over the summit was very short. The existence of cold-based Laurentide ice has been documented widely in the high latitudes ADDIN EN.CITE (Briner et al., 2014; Briner et al., 2006; Corbett et al., 2016a; Margreth et al., 2016) and also in the contiguous United States, including the low elevations of Wisconsin (Bierman et al., 1999; Colgan et al., 2002) and the highest summits of Maine and New Hampshire (Bierman et al., 2015). In this case, the summit regions of Mt. Mansfield (and other mountains of the northeastern United States) may represent relict landscapes that were preserved, but not deeply eroded or reshaped, beneath LGM ice cover ADDIN EN.CITE (Sugden, 1977, 1978; Sugden and Watts, 1977). The soils on the summit of Mt. Mansfield, which preserve evidence of significant contribution from dust (Munroe et al., 2007), may predate the Holocene if they were preserved subglacially. The presence of old, longexposed soils is consistent with the observation that sediments from the Brown's River, which drains Mt. Mansfield's western flank, have appreciably higher meteoric ¹⁰Be concentrations

than other river sediments in Vermont (Borg, 2010).

374

375

6.3. Regional Deglaciation History and Dynamics

376

377

378

379

380

381

382

383

384

385

386

387

388

389

390

Our findings, in context of regional data, show that the LIS margin advance and retreat rates appear to have been different and the duration of LGM ice cover over Mt. Mansfield was short, consistent with minimal and spatially variable erosion on the summit. As late Pleistocene climate cooled, the advancing LIS margin may not have reached southern Quebec until 31270 \pm 200 or 33250 \pm 240 14 C yr BP (34440 or 36350 cal yr BP, using the MARINE13 calibration curve and a 400 yr marine reservoir correction) based on ages of fossiliferous Champlain Sea marine sediments later over-run by ice (Parent and Dube-Loubert, 2017). The LIS margin occupied its terminal position ~500 km to the south at or until ~27.6 ka (Martha's Vineyard; Balco et al. (2002)) and ~25.5 ka (New Jersey; Corbett et al. (2017)) (both recalculated as described above), representing an advance that took ~9 ka (assuming the interval between 35.4 and 26.6 ka, the averages of the above pairs of ages, which is a maximum estimate if the dated boulders were deposited during moraine abandonment). During deglaciation, the retreating LIS margin did not retreat to southern Quebec until $\sim 11^{14}$ C ka BP (~ 13 cal ka BP, Richard and Occhietti (2005)), retreating across the 500 km span over ~13 ka, considerably longer than it took to advance across the same distance.

391

392

393

394

These estimates imply that advance occurred more rapidly than retreat. This observation is consistent with recent sea level reconstructions that indicate rapid fall at the beginning of the glacial period and less rapid rise at the end of glaciation (Lambeck et al., 2014; Siddall et al., 2008). Conversely, it is also possible that an Appalachian Ice Dome existed, with

spreading centers in the highland areas of northern New England as postulated by Flint (1951), which would explain why ice margin advance appears to have occurred so quickly. Regardless, the retreat rate (and probably also the advance rate) was heterogeneous according to varve chronology (Ridge et al., 2012), occurring rapidly in certain areas and slowly in other areas, ranging across an order of magnitude from several tens to several hundreds of m yr⁻¹.

Under the above assumptions, Mt. Mansfield would have been covered for a maximum of ~21.5 ka (from 35.4 ka based on Parent and Dube-Loubert (2017) to 13.9 ka based on ¹⁰Be). However, the duration could have been shorter since the estimates of LIS advance are from low -elevation areas ~75 km to the north of Mt. Mansfield, or the duration could have been longer depending on how much time elapsed before the ice to thickened sufficiently to cover Mt. Mansfield's middle elevations. For the lower elevations, where inherited ¹⁰Be does not exist in appreciable quantities in our samples, at least several meters of material (or possibly much more) was eroded from rock surfaces during the duration of LIS cover. This rock removal represents a minimum subglacial erosion rate of ~0.1 m kyr⁻¹, assuming 2 m over 20 ka, although erosion rates could have been much higher if the duration of cover was shorter and/or the erosion depth greater.

The timing of LIS retreat from Mt. Mansfield as constrained with 10 Be (13.9 \pm 0.6 ka) is generally consistent with retreat constraints from other deglacial chronologies in the northeastern United States. The North American Varve Chronology (Ridge et al., 2012) suggests that the LIS margin was at the latitude of Mt. Mansfield around this time (Fig. 1). This temporal overlap implies a minimal time lag between exposure of the uplands and of the valleys; the duration of time during which channelized ice flow occurred only through the valleys, leaving

the summits exposed as nunataks, was probably at most hundreds of years to a millennium.

Organic 14 C ages from lake and pond sediment core bottoms paint a complex picture of deglaciation timing in northern New England (Fig. 1), likely due to inaccuracies associated with old carbon in bulk ages and/or an uncertain lag time between deglaciation and the deposition of organic material. The 10 Be age we infer for exposure of Mt. Mansfield's middle and low elevations (13.9 \pm 0.6 ka) disagrees at 1σ (although agrees within 2σ) with the nearby minimum -limiting basal age of 15200 cal yr BP from Sterling Pond (Lin, 1996); however, the latter is from bulk sediment and is older than most organic 14 C ages in the area, and thus we suspect it contains older, reworked carbon. The age we infer using 10 Be is generally consistent with the LIS margin reconstructions of Dyke (2004), which are based on a compilation of North American, subarctic, and arctic organic 14 C ages, and place the retreating LIS margin in central/northern Vermont at \sim 14.4 cal ka BP.

Field observations provide additional information about ice thinning dynamics. Glacial striations preserved on Mount Mansfield (Fig. 2) were produced during several different ice flow regimes. Those oriented NW-SE were produced when the ice was thick enough to flow obliquely across the mountains; this striation orientation is found elsewhere along the crest of the Green Mountains and at high-elevation sites across New England (Wright, 2015). A limited area where striations are oriented NE-SW indicates a period of ice flow into the Champlain valley possibly in response to an ice-streaming event similar to an earlier and larger-scale event documented in the southern Champlain and northern Hudson valleys (Wright, 2015, 2017).

Striations oriented N-S were produced when the ice sheet thinned sufficiently that its flow was topographically controlled by the north-south valleys that border the Green Mountains. These

observations are consistent with previous conceptual models of LIS deglaciation that argued for thinning, channelization, and active flow through the valleys during retreat (for a review, see Koteff and Pessl (1981)).

The existence of glacial Lake Winooski (Fig. 1), which flanks Mt. Mansfield to the east, indicates that once the ice sheet thinned sufficiently to become topographically controlled, deglaciation of the northern Green Mountains was very asymmetric. Glacial Lake Winooski on the east side of the mountains formed while a tongue of the ice sheet west of the mountains dammed the Winooski River valley (Wright, 2001), showing that ice on the east side of the mountains retreated earlier and perhaps faster than ice in the Champlain Valley to the west. Over the lake's ~280-year history, the ice sheet margin on the east side of the mountains rapidly retreated at an average rate of ~240 m yr⁻¹ before it began to drain (Wright, 2001).

The small ridges visible on Mt. Mansfield's eastern and western flanks (Fig. 2) may be annual moraines formed by small seasonal oscillation of the waning LIS margin. The elevation spans of several well-preserved sequences of moraines (7 to 22 moraines) on the eastern flank of the mountain indicates average elevation drops between adjacent moraines of 9 to 23 m (Wright, 2018). If these moraines are indeed annual features, then the ice sheet was thinning between 9 and 23 m yr⁻¹, and the amount of time necessary to expose the 800 m vertical span of our samples is ~35-90 years. This field-based evidence of rapid thinning aligns well with our ¹⁰Be chronology, which suggests that thinning occurred faster than the resolution of the ¹⁰Be chronometer.

Conclusions

In situ cosmogenic 10 Be and 14 C data, as well as field observations of striation directions and moraine crests, sheds light on differing histories and processes between the low and high elevations at Mt. Mansfield. The lower elevations were characterized by significant glacial erosion during the LGM and rapid ice thinning at 13.9 ± 0.6 ka, which exposed areas between \sim 400 and 1200 m a.s.l. simultaneously within the resolution of the 10 Be chronometer. The higher elevations were characterized by inefficient glacial erosion during LGM ice cover, leading to the preservation of surfaces subglacially. The summit remained at least partially covered by snowfields, ice carapaces, and/or till that persisted until the early Holocene. Our data suggest that as the LIS thinned rapidly, ice became confined to the valleys, allowing channelized flow to lag deglaciation of the uplands by centuries; stripping of the summit to expose bare bedrock lagged deglaciation by millennia.

Acknowledgements

This work was funded by NSF-EAR 1603175 to J. Shakun and NSF-EAR 1602280 to P. Bierman.

Cosmogenic samples were prepared with laboratory support from NSF-EAR 1735676 to P.

Bierman.

Table Captions

- Table 1. Compilation of previous work relevant to Mt. Mansfield's deglacial history.
- Table 2. Sample location information and field data for 20 bedrock and boulder samples from Mt. Mansfield.
- Table 3. Sample preparation and laboratory information for ¹⁰Be/⁹Be analyses.
- Table 4. Sample preparation and laboratory information for $^{14}\text{C}/^{12}\text{C}$ analyses.
- Table 5. Calculated exposure ages based on in situ 10 Be (n = 20) and 14 C (n = 3) concentrations.

Figure Captions

Figure 1. Generalized map of northern New York, Vermont, and New Hampshire showing previous age constraints (in ka) relevant to Mt. Mansfield's deglacial history. Ice margin positions based on glacial Lake Hitchcock varve chronology in the Connecticut River valley from Ridge et al. (2012) are shown in thick black lines. Radiocarbon ages from multiple studies are shown with black circles and are detailed in Table 1. The extents of glacial lakes are shown in light gray. The black box shows the location of Figure 4, and Mt. Mansfield is shown by the black triangle. The inset shows the location of the study area in relation to the northeastern United States and southeastern Canadian provinces, with the LIS maximum extent shown in the heavy black line.

Figure 2. Shaded relief map of the Mt. Mansfield area based on LiDAR, with 100 m contours shown in black (LiDAR from the Vermont Center for Geographic Information, www.vcgi. vermont.gov). Thin arrows denote striation measurements and white dashed lines show mapped moraine crests. Sample sites are shown with white circles (refer to Figure 4 for sample names).

Figure 3. Photographs from the study area. A: A typical middle-elevation surface exhibiting subtle rounding (location of sample MM-15, 1025 m a.s.l.). B: A typical higher-elevation surface exhibiting frost shattering (location of sample MM-08, 1305 m a.s.l.). C: Sampling boulder MM-04, which sits on top of a pavement outcrop (1174 m a.s.l.). D: Fractured bedrock (location of sample MM-06, 1197 m a.s.l.). E: A rounded outcrop partway down Sunset Ridge on Mt. Mansfield's west side (location of sample MM-13, 1174 m a.s.l.). F: Our attempt at rephotographing the iconic boulder shown in Hitchcock et al. (1861), which became sample MM-03 (1176 m a.s.l.).

Figure 4. Satellite imagery (Google Earth) of the Mt. Mansfield area (see location context in Figs. 1 and 2). Sample locations are shown with white circles (bedrock) and gray circles (boulders). All ages (in ka, detailed in Table 5) are 10 Be unless otherwise specified; uncertainties are 1σ internal.

Figure 5. Exposure ages (calculated assuming no inherited nuclides and no post-burial shielding or erosion) shown against elevation. Round symbols show boulders and square symbols show bedrock; gray symbols show ^{10}Be and hollow symbols show in situ ^{14}C . Error bars show 1σ internal uncertainties, which in many cases are smaller than the symbols.

Figure 6. $^{14}\text{C}/^{10}\text{Be}$ two-isotope plot modified from the CRONUS calculator output. Production rates for both nuclides have been normalized to 1 to account for spatially variable production, particularly muon production. The top curve shows the continuous exposure and production pathway, while the bottom curve defines the bottom of the erosion envelope. Error ellipses are 1σ .

Figure 7. Simulated June/July/August daily average freezing level for $44 \circ N$ $72 \circ W$ from Liu et al. (2009), courtesy of F. He. Overlain in gray bars are inferences from the cosmogenic data described in the text.

Location ^a	Map Code	Latitude (°N)	Longitude (°E)	Elevation (m)	Material Type ^b	Radiocarbon Age and Uncertainty (yr)	Calibrated Age and Uncertainty (yr) ^c	Reference
(B) Beecher Pond, VT	BP	44.812006	-71.849973	375	Single plant macrofossil (A) 9810 ± 55 11230 (11190-11250) Munroe		Munroe (2012)	
(B) Bugbee Bog, VT	BB	44.367348	-72.159139	400	Bulk sediment (D)	11030 ± 200	12920 (12740-13060)	McDowell et al. (1971)
(B) Chapel Pond, NY	CP	44.139383	-73.747337	500	Single plant macrofossil (A)	9970 ± 50	11410 (11270-11600)	Noren et al. (2002)
(B) Crystal Lake, NH	CL	43.909736	-71.075430	145	Single plant macrofossil (A)	11350 ± 330	13210 (12840-13480)	Parris et al. (2010)
(B) Deer Lake Bog, NH	DLB	44.029705	-71.826551	1325	Bulk sediment (D)	13000 ± 400	15490 (14900-16200)	Spear (1989)
(B) Duck Pond, VT	DP	44.708443	-72.066322	520	Single plant macrofossil (A)	10930 ± 40	12780 (12730-12810)	Noren et al. (2002)
(B) Eagle Lake Bog, NH	ELB	44.160612	-71.658790	1265	Bulk sediment (D)	9155 ± 145	10350 (10190-10540)	Spear (1989)
(V) Elizabethtown, NY	E	44.208696	-73.498219	188	Musk ox bone (A)	11360 ± 115	13210 (13100-13300)	Cadwell et al. (1991); Rayburn et al. (2007)
(B) Heart Lake, NY	HL	44.182813	-73.968740	665	Bulk sediment (D)	10475 ± 230	12280 (12040-12670)	Whitehead and Jackson (1990)
(B) Lake Morey, VT	LM	43.921449	-72.152912	125	Single plant macrofossil (A)	10180 ± 100	11850 (11620-12060)	Noren et al. (2002)
(B) Lake of the Clouds, NH	LC	44.258129	-71.317390	1535	Bulk sediment (D)	11530 ± 420	13420 (12900-13800)	Spear (1989)
(B) Lonesome Lake, NH	LL	44.139728	-71.701652	830	Bulk sediment (D)	10535 ± 495	12220 (11500-12880)	Spear et al. (1994)
(V) Long Pond, NY	LNP	44.390155	-73.452430	180	Wood fragment (A)	10900 ± 75	12780 (12710-12830)	Rayburn et al. (2007)
(B) Lost Pond, NH	LSP	44.249822	-71.250710	635	Bulk sediment (D)	12870 ± 370	15290 (14710-15960)	Spear et al. (1994)
(B) Nulhegan Pond, VT	NP	44.790682	-71.818026	355	Single plant macrofossil (A)	9750 ± 50	11190 (11160-11230)	Munroe (2012)
(B) Pond of Safety, NH	PS	44.410191	-71.341568	680	Assorted plant macrofossils (A)	12450 ± 60	14590 (14340-14770)	Thompson et al. (1996)
(B) Profile Lake, NH	PL	44.163804	-71.677561	590	Bulk sediment (A)	10660 ± 40	12640 (12600-12680)	Rogers et al. (2009)
(B) Ritterbush Pond, VT	RP	44.746654	-72.599735	315	Bulk sediment (D)	10730 ± 200	12620 (12400-12850)	Sperling et al. (1989)
(B) Ritterbush Pond, VT	RP	44.746654	-72.599735	315	Bulk sediment (A)	12020 ± 90	13880 (13760-13980)	Lin (1996)
(B) Ritterbush Pond, VT	RP	44.746654	-72.599735	315	Bulk gyttja (A)	11940 ± 90	13780 (13610-13930)	Bierman et al. (1997)
(B) South Pond, NH	SOP	44.594110	-71.362365	340	Single plant macrofossil (A)	11825 ± 40	13650 (13600-13710)	Parris et al. (2010)
(B) Sterling Pond, VT	SEP	44.556175	-72.774341	920	Bulk sediment (A)	12760 ± 70	15200 (15100-15300)	Lin (1996)
(B) Stinson Lake, NH	SL	43.868145	-71.799527	395	Single plant macrofossil (A)	12345 ± 45	14340 (14160-14460)	Parris et al. (2010)
(B) Upper Wallface Pond, NY	UWP	44.148239	-74.056049	955	Bulk sediment (D)	12390 ± 480	14590 (13800-15210)	Whitehead and Jackson (1990)

 $^{^{}a}(B)\ denotes\ a\ basal\ age\ of\ a\ sediment\ core\ from\ a\ small\ upland\ lake\ or\ pond;\ (V)\ denotes\ an\ age\ of\ glacial\ Lake\ Vermont\ sediments.$

Table 1.

^b(A) denotes an age obtained by Accelerator Mass Spectrometry; (D) denotes an age obtained by decay counting.

 $^{^{}c}$ Ages were calibrated using the Calib program version 7.1 (Stuiver et al., 2015) and the IntCal13 calibration curve (Reimer et al., 2013). The calibrated age shows the median probability, with the 1σ age range in parentheses.

Sample Name	Type	Latitude (°N)	Longitude (°E)	Elevation (m a.s.l.)	Sample Thickness (cm)	Rock Type
MM-01	Boulder	44.530	-72.817	1164	3.0	Schist
MM-02	Bedrock	44.531	-72.817	1172	1.0	Schist
MM-03	Boulder	44.534	-72.817	1176	2.5	Schist
MM-04	Boulder	44.533	-72.817	1174	5.0	Schist
MM-05	Bedrock	44.535	-72.817	1180	1.5	Schist
MM-06	Bedrock	44.536	-72.817	1197	1.0	Schist
MM-07	Bedrock	44.536	-72.817	1197	1.5	Schist
MM-08	Bedrock	44.544	-72.814	1305	1.5	Schist
MM-09	Bedrock	44.543	-72.815	1300	2.0	Schist
MM-10	Bedrock	44.543	-72.816	1297	1.5	Schist
MM-11	Bedrock	44.542	-72.815	1270	2.0	Schist
MM-12	Bedrock	44.544	-72.818	1226	2.5	Schist
MM-13	Bedrock	44.544	-72.821	1174	2.0	Schist
MM-14	Bedrock	44.543	-72.823	1090	2.0	Schist
MM-15	Bedrock	44.542	-72.826	1025	1.0	Schist
MM-16	Boulder	44.519	-72.830	923	2.0	Schist
MM-17	Bedrock	44.519	-72.831	903	2.5	Quartz vein
MM-19	Boulder	44.524	-72.827	826	3.5	Granite
MMB-02	Boulder	44.506	-72.858	409	2.0	Gneiss
MMB-03	Boulder	44.506	-72.861	411	2.0	Gneiss

Table 2.

Sample Name	Preparation Group ^a	Quartz Mass (g)	Mass of ⁹ Be Added (μg)	Cathode	Measured 10Be/Be Ratio	Measured 10 Be/Be Ratio Uncertainty	Background- Corrected 10Be/Be Ratio ^c	Background- Corrected 10 Be/Be Ratio Uncertainty ^c	¹⁰ Be Concentration (atoms g ⁻¹)	¹⁰ Be Concentration Uncertainty (atoms g ⁻¹)
MM-01	A	21.6956	248.3	BE41216	2.03E-13	3.94E-15	2.02E-13	3.97E-15	1.54E+05	3.03E+03
MM-02	Α	21.9757	248.3	BE41217	2.20E-13	4.87E-15	2.19E-13	4.89E-15	1.65E+05	3.68E+03
MM-03	Α	22.8944	247.4	BE41218	2.10E-13	4.07E-15	2.09E-13	4.10E-15	1.50E+05	2.95E+03
MM-04	Α	22.3445	247.9	BE41220	2.01E-13	3.91E-15	2.00E-13	3.93E-15	1.48E+05	2.91E+03
MM-05	A	22.8325	247.4	BE41221	2.11E-13	4.09E-15	2.10E-13	4.12E-15	1.52E+05	2.98E+03
MM-06	Α	22.3709	247.9	BE41222	2.18E-13	4.23E-15	2.17E-13	4.25E-15	1.60E+05	3.14E+03
MM-07	Α	21.2423	247.0	BE41223	2.00E-13	4.34E-15	1.99E-13	4.36E-15	1.54E+05	3.38E+03
MM-08	A	23.4842	247.3	BE41224	3.11E-13	5.88E-15	3.10E-13	5.89E-15	2.17E+05	4.14E+03
MM-09	Α	22.2638	247.1	BE41226	3.90E-13	7.49E-15	3.89E-13	7.51E-15	2.88E+05	5.55E+03
MM-10	Α	22.4876	245.2	BE41227	2.75E-13	6.46E-15	2.74E-13	6.48E-15	1.99E+05	4.71E+03
MM-11	A	22.5446	248.9	BE41253	2.47E-13	4.68E-15	2.46E-13	4.70E-15	1.80E+05	3.45E+03
MM-12	A	22.5105	248.7	BE41254	2.81E-13	6.05E-15	2.80E-13	6.07E-15	2.06E+05	4.45E+03
MM-13	Α	22.7827	249.0	BE41255	2.20E-13	4.19E-15	2.19E-13	4.21E-15	1.59E+05	3.06E+03
MM-14	Α	22.5454	248.7	BE41256	1.90E-13	5.76E-15	1.89E-13	5.78E-15	1.38E+05	4.23E+03
MM-15	A	22.4397	248.4	BE41257	1.87E-13	3.56E-15	1.86E-13	3.59E-15	1.37E+05	2.64E+03
MM-16	В	19.9998	240.4	148329	1.41E-13	5.40E-15	1.40E-13	5.40E-15	1.13E+05	4.34E+03
MM-17	В	20.7278	241.4	148327	1.61E-13	5.39E-15	1.61E-13	5.39E-15	1.25E+05	4.19E+03
MM-19	В	21.3233	240.7	148324	1.37E-13	4.44E-15	1.36E-13	4.45E-15	1.03E+05	3.35E+03
MMB-02	В	19.0157	241.9	150356	9.31E-14	3.89E-15	9.24E-14	3.89E-15	7.85E+04	3.31E+03
MMB-03	В	20.2968	243.4	147146	9.63E-14	3.81E-15	9.56E-14	3.81E-15	7.66E+04	3.06E+03
		9								9

^aGroup A: Prepared in 2016, ⁹Be carrier concentration of 299 μg mL¹, analysis at Lawrence Livermore National Laboratory. Group B: Prepared in 2017-2018, ⁹Be carrier concentration of 291 μg mL¹, analysis at Purdue Rare Isotope Measurement Laboratory.

Table 3.

^bRatios were normalized against standard 07KNSTD3110 with an assumed ratio of 2.850 x 10⁻¹² (Nishiizumi et al., 2007).

 $[^]c$ Measured ratios were corrected for backgrounds using the average of blanks prepared with the samples and measured at the same AMS. Preparation group A: n = 4 analyzed at Lawrence Livermore National Laboratory, $1.08 \pm 0.46 \times 10^{-15}$. Group B: n = 4 analyzed at Purdue Rare Isotope Measurement Laboratory, $0.74 \pm 0.20 \times 10^{-15}$ (average ± 1 SD). Background-corrected uncertainties include sample measurement uncertainty and blank uncertainty propagated in quadrature.

Sample Name	Quartz Mass (g)	Total C Yield (mg)	Diluted C Mass (mg)	AMS Cathode Number	Mesured ¹⁴ C/ ¹³ C Ratio ^a	Measured ¹⁴ C/ ¹³ C Ratio Uncertainty ^a	Measured 14C/C Ratio ^a	Measured ¹⁴ C/C Ratio Uncertainty ^a	¹⁴ C Concentration (atoms g ⁻¹)	Concentration Uncertainty (atoms g ⁻¹)
MM-03	3.0095	40.7	107.2	OS-135188	1.407E-11	6.875E-14	1.539E-13	7.604E-16	2.432E+05	4.037E+03
MM-08	3.0015	11.3	103.9	OS-135189	1.436E-11	7.810E-14	1.576E-13	8.788E-16	2.417E+05	4.024E+03
MM-09	3.0392	8.7	107.4	OS-135192	1.282E-11	8.678E-14	1.410E-13	9.569E-16	2.184E+05	3.750E+03

 $^{^{}a}$ Ratios were normalized against standard Ox-II with an assumed 14 C/ 13 C ratio of 1.4575 x 10^{-10} .

Table 4.

Sample Name	Туре	Elevation (m a.s.l.)	¹⁰ Be Exposure Age (ka) ^a	¹⁰ Be Internal Uncertainty (ka) ^a	¹⁰ Be External Uncertainty (ka) ^a	¹⁴ C Exposure Age (ka) ^a	¹⁴ C Internal Uncertainty (ka) ^a	¹⁴ C External Uncertainty (ka) ^a
MM-01	Boulder	1164	14.49	0.29	1.24			
MM-02	Bedrock	1172	14.82	0.33	1.28			
MM-03	Boulder	1176	13.65	0.27	1.17	15.64	0.85	2.48
MM-04	Boulder	1174	13.75	0.27	1.18			
MM-05	Bedrock	1180	13.61	0.27	1.16			
MM-06	Bedrock	1197	14.10	0.28	1.21			
MM-07	Bedrock	1197	13.63	0.30	1.17			
MM-08	Bedrock	1305	17.43	0.33	1.49	11.69	0.47	1.37
MM-09	Bedrock	1300	22.90	0.45	1.96	9.67	0.35	0.98
MM-10	Bedrock	1297	16.15	0.38	1.40			
MM-11	Bedrock	1270	15.02	0.29	1.28			
MM-12	Bedrock	1226	17.78	0.39	1.53			
MM-13	Bedrock	1174	14.44	0.28	1.23			
MM-14	Bedrock	1090	13.52	0.42	1.20			
MM-15	Bedrock	1025	13.98	0.27	1.20			
MM-16	Boulder	923	13.13	0.51	1.21			
MM-17	Bedrock	903	15.20	0.51	1.37			
MM-19	Boulder	826	12.85	0.42	1.15			
MMB-02	Boulder	409	13.99	0.59	1.31			
MMB-03	Boulder	411	13.61	0.55	1.26			

^aAll cosmogenic ages were calculated using Version 3 of the CRONUS Earth Online Exposure Age Calculator (Balco et al., 2008) and the Northeastern North American production rate (Balco et al., 2009) with LSDn scaling.

Table 5.

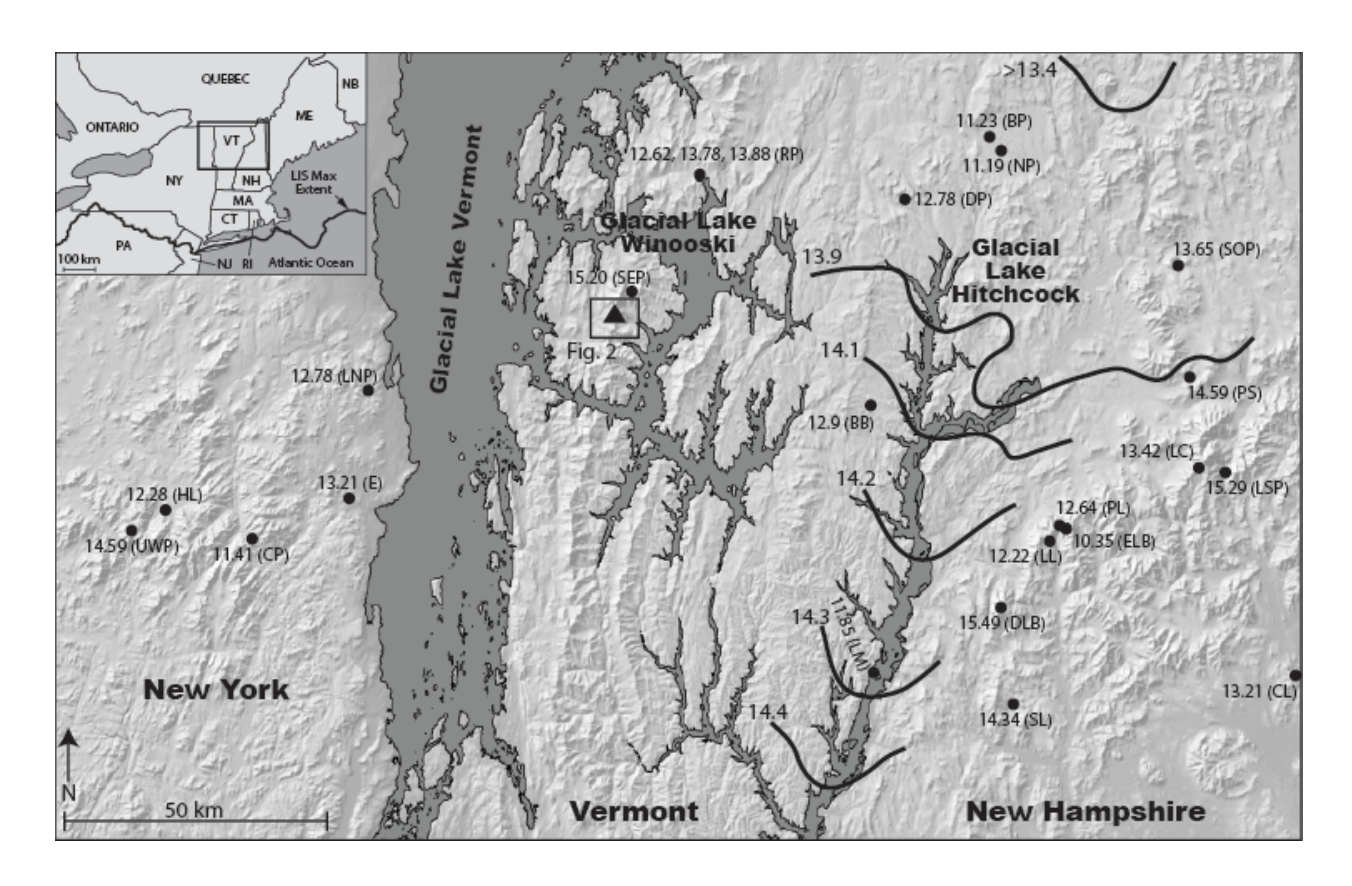


Figure 1.

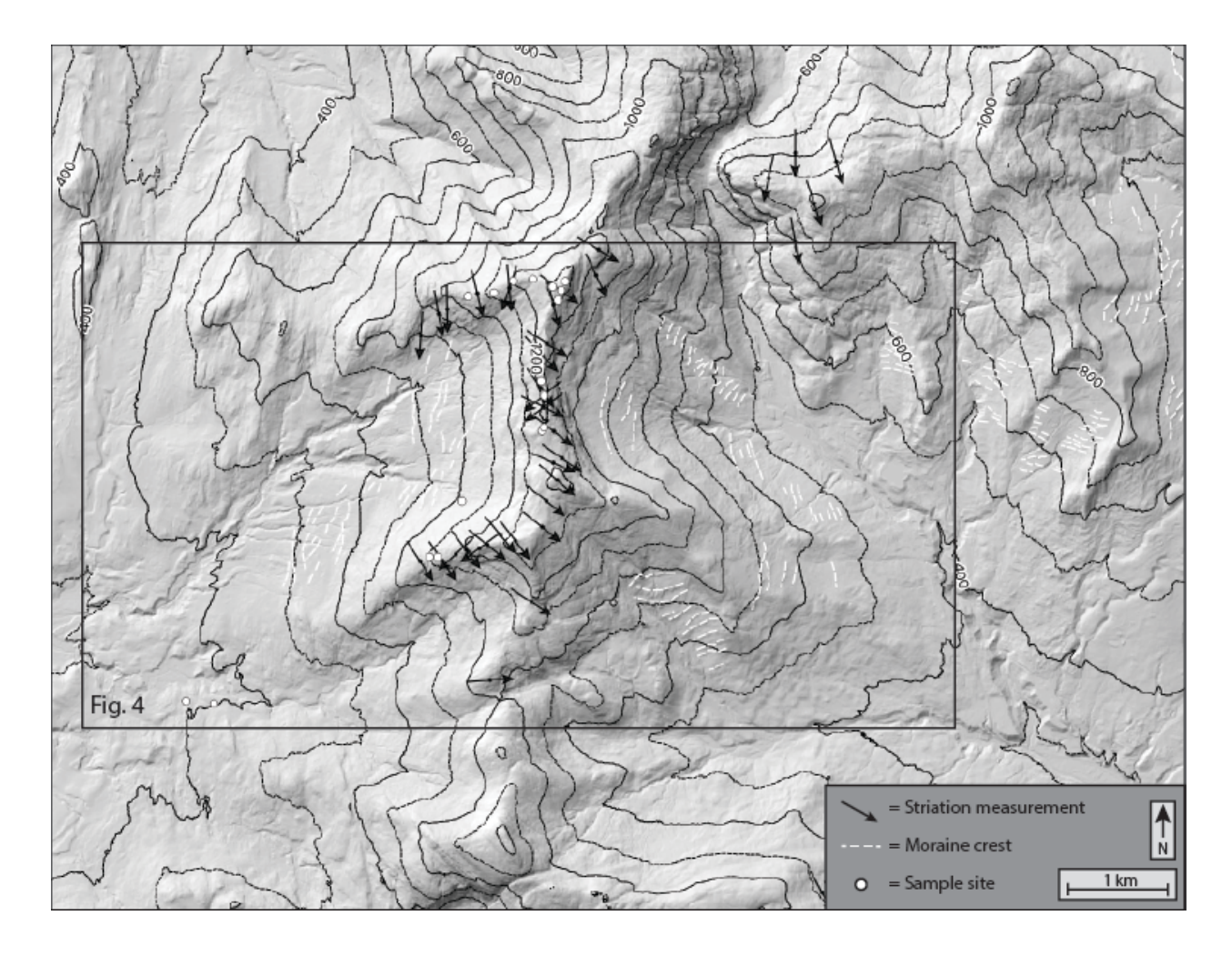


Figure 2.

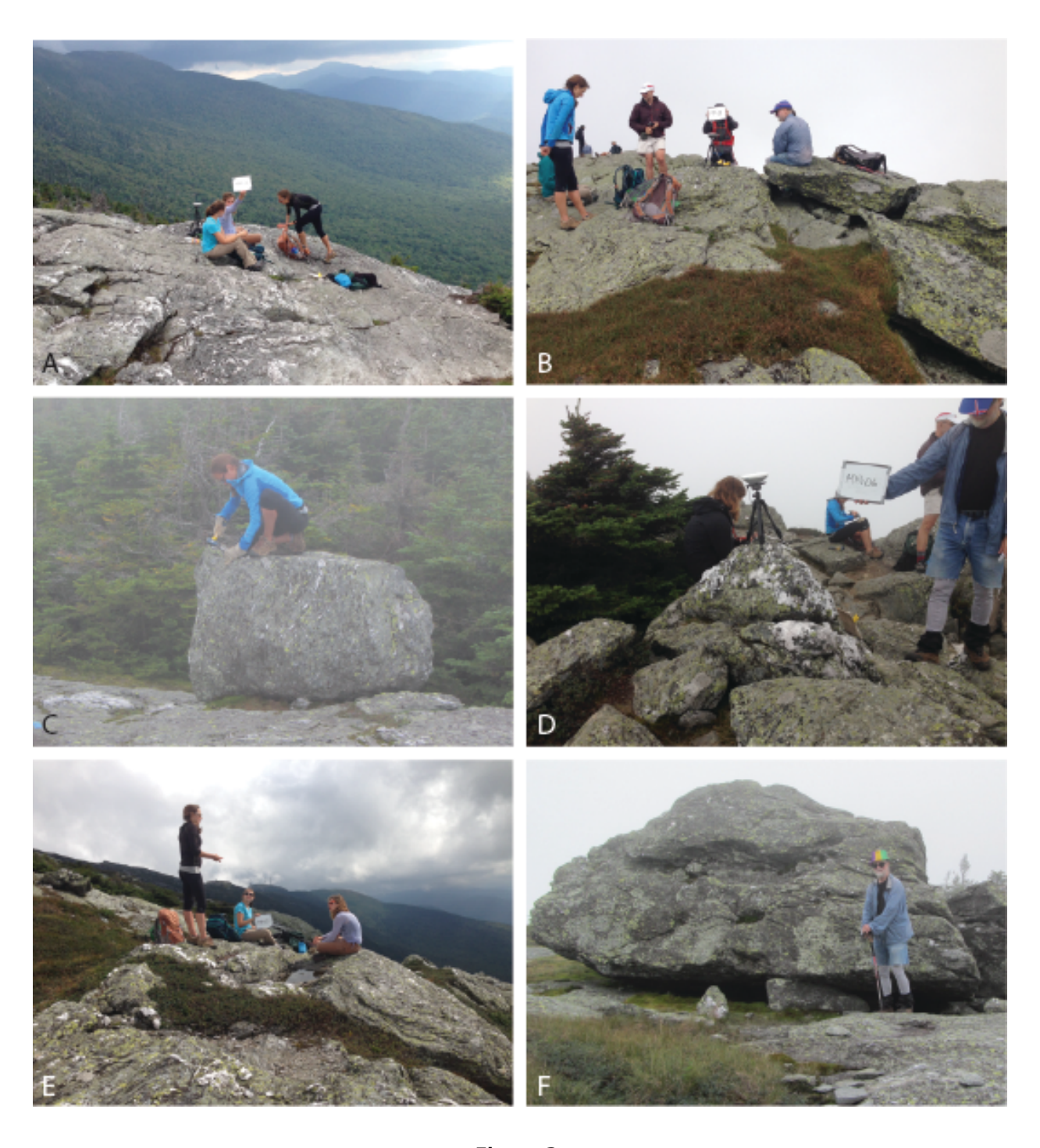


Figure 3.

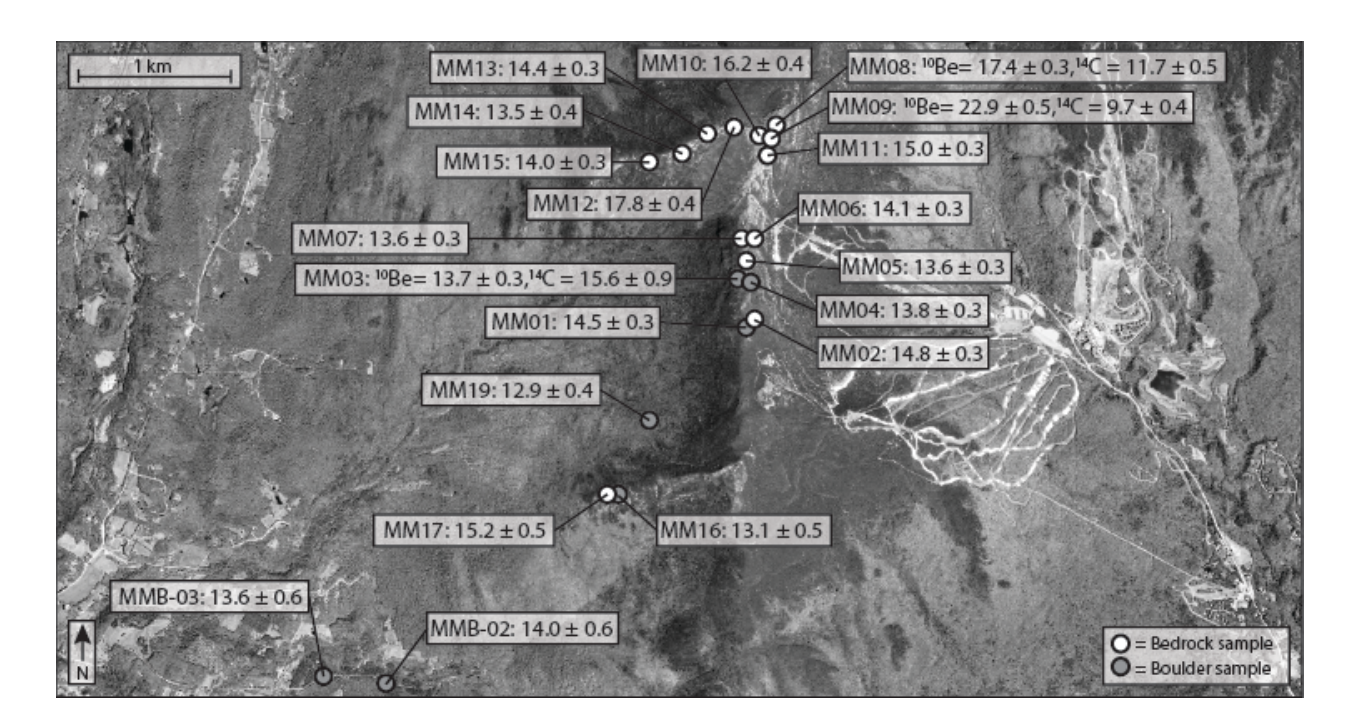


Figure 4.

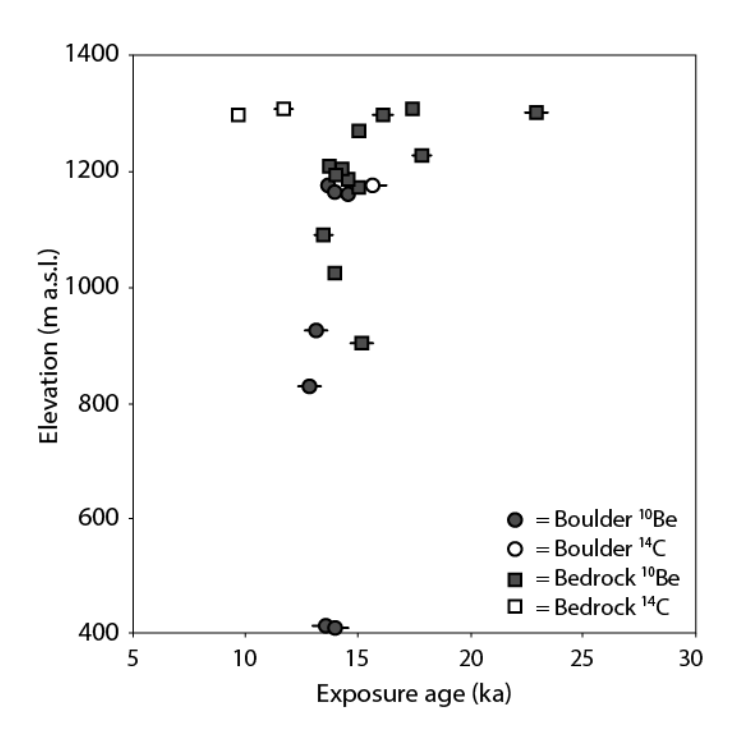


Figure 5.

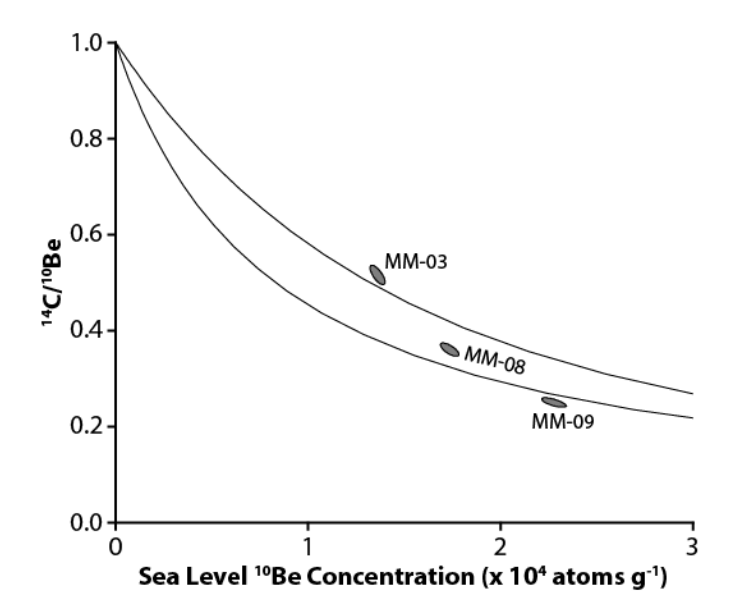


Figure 6.

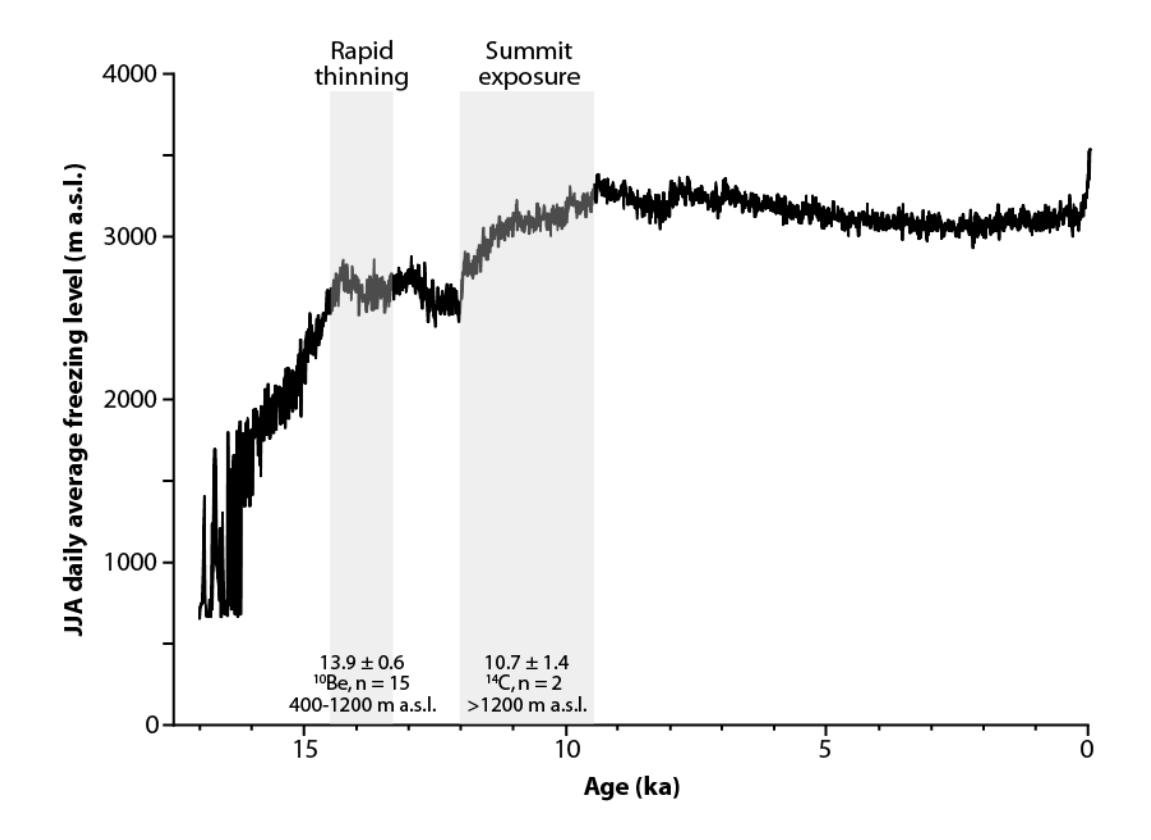


Figure 7.

References

- ADDIN EN.REFLIST Balco, G., 2011. Contributions and unrealized potential contributions of cosmogenic-nuclide exposure dating to glacier chronology, 1990-2010. Quaternary Science Reviews 30, 3-27.
- Balco, G., Briner, J., Finkel, R.C., Rayburn, J.A., Ridge, J.C., Schaefer, J.M., 2009. Regional beryllium-10 production rate calibration for late-glacial northeastern North America. Quaternary Geochronology 4, 93-107.
- Balco, G., Schaefer, J., 2006. Cosmogenic-nuclide and varve chronologies for the deglaciation of southern New England. Quaternary Geochronology 1, 15-28.
- Balco, G., Stone, J.O., Lifton, N.A., Dunai, T.J., 2008. A complete and easily accessible means of calculating surface exposure ages or erosion rates from ¹⁰Be and ²⁶Al measurements. Quaternary Geochronology 3, 174-195.
- Balco, G., Stone, J.O.H., Porter, S.C., Caffee, M.W., 2002. Cosmogenic-nuclide ages for New England coastal moraines, Martha's Vineyard and Cape Cod, Massachusetts, USA. Quaternary Science Reviews 21, 2127-2135.
- Bierman, P.R., 1994. Using in situ produced cosmogenic isotopes to estimate rates of landscape evolution: A review from the geomorphic perspective. Journal of Geophysical Research 99, 13885-13896.
- Bierman, P.R., Davis, P.T., Corbett, L.B., Lifton, N.A., 2015. Cold-based, Laurentide ice covered New England's highest summits during the Last Glacial Maximum. Geology 43, 1059-1062.
- Bierman, P.R., Lini, A., Zehfuss, P., Church, A., Davis, P.T., Southon, J., Baldwin, L., 1997.

 Postglacial Ponds and Alluvial Fans: Recorders of Holocene Landscape History. GSA
 Today 7, 1-8.
- Bierman, P.R., Marsella, K.A., Patterson, C., Davis, P.T., Caffee, M., 1999. Mid-Pleistocene cosmogenic minimum-age limits for pre-Wisconsinan glacial surfaces in southwestern Minnesota and southern Baffin Island: a multiple nuclide approach. Geomorphology 27, 25-39.
- Borchers, B., Marrero, S., Balco, G., Caffee, M., Goehring, B., Lifton, N., Nishiizumi, K., Phillips, F., Schaefer, J., Stone, J., 2016. Geological calibration of spallation production rates in the CRONUS-Earth project. Quaternary Geochronology 31, 188-198.
- Borg, J., 2010. Streambank stability and sediment tracing in Vermont waterways, Civil and Environmental Engineering. University of Vermont, Burlington, VT, p. 110.
- Briner, J.P., Bini, A.C., Anderson, R.S., 2009. Rapid early Holocene retreat of a Laurentide outlet glacier through an Arctic fjord. Nature Geoscience 2, 496-499.
- Briner, J.P., Goehring, B.M., Mangerud, J., Svendsen, J.I., 2016. The deep accumulation of ¹⁰Be at Utsira, southwestern Norway: Implications for cosmogenic nuclide exposure dating in peripheral ice sheet landscapes. Geophysical Research Letters 43, 9121-9129.
- Briner, J.P., Lifton, N.A., Miller, G.H., Refsnider, K., Anderson, R., Finkel, R., 2014. Using in situ cosmogenic ¹⁰Be, ¹⁴C, and ²⁶Al to decipher the history of polythermal ice sheets on Baffin Island, Arctic Canada. Quaternary Geochronology 19, 4-13.
- Briner, J.P., Miller, G.H., Davis, P.T., Finkel, R.C., 2005. Cosmogenic exposure dating in arctic glacial landscapes: implications for the glacial history of northeastern Baffin Island,

- Arctic Canada. Canadian Journal of Earth Sciences 42, 67-84.
- Briner, J.P., Miller, G.H., Davis, P.T., Finkel, R.C., 2006. Cosmogenic radionuclides from fjord landscapes support differential erosion by overriding ice sheets. Geological Society of America Bulletin 118, 406-420.
- Bromley, G.R.M., Hall, B.L., Thompson, W.B., Kaplan, M.R., Hgarcia, J.L., Schaefer, J.M., 2015. Late glacial fluctuations of the Laurentide Ice Sheet in the White Mountains of Maine and New Hampshire, U.S.A. Quaternary Research 83, 522-530.
- Brown, S.L., 1999. Terrestrial sediment deposition in Ritterbush Pond: Implications for Holocene storm frequency in northern Vermont, Geology. University of Vermont, Burlington, VT, p . 180.
- Buizert, C., Gkinis, V., Severinghaus, J.P., He, F., Lecavalier, B.S., Kindler, P., Leuenberger, M., Carlson, A.E., Vinther, B., Masson-Delmotte, V., White, J.W.C., Liu, Z., Otto-Bliesner, B.L., Brook, E.J., 2014. Greenland temperature response to climate forcing during the last deglaciation. Science 345, 1177-1180.
- Cadwell, D.H., Connally, G.G., Dineen, R.J., Fleisher, P.J., Franzi, D.A., Fuller, M.L., Gurrieri, J.T., Haselton, G.M., Kelley, G.C., LaFleur, R.G., Muller, E.H., Pair, D.L., Rich, J.L., Sirkin, L.A., Young, R.A., Wiles, G.C., 1991. Surficial geology map of New York, New York State Museum Map and Chart Series 40, 1:125,000.
- Chapman, D.H., 1937. Late-glacial and postglacial history of the Champlain Valley. American Journal of Science, 89-124.
- Christman, R.A., 1959. Geology of the Mount Mansfield Quadrangle, Vermont. Bulletin No. 12 of the Vermont Geological Survey, 75.
- Clark, P.U., Marshall, S.J., Clarke, G.K.C., Hostetler, S.W., Licciardi, J.M., Teller, J.T., 2001.

 Freshwater forcing of abrupt climate change during the Last Glaciation. Science 293, 283
 -287.
- Colgan, P.M., Bierman, P.R., Mickelson, D.M., Caffee, M., 2002. Variation in glacial erosion near the southern margin of the Laurentide Ice Sheet, south-central Wisconsin, USA:

 Implications for cosmogenic dating of glacial terrains. Geological Society of America Bulletin 114, 1581-1591.
- Corbett, L.B., Bierman, P.R., Davis, P.T., 2016a. Glacial history and landscape evolution of southern Cumberland Peninsula, Baffin Island, Canada, constrained by cosmogenic ¹⁰Be and ²⁶Al. Geological Society of America Bulletin 128, 1173-1192.
- Corbett, L.B., Bierman, P.R., Graly, J.A., Neumann, T.A., Rood, D.H., 2013. Constraining landscape history and glacial erosivity using paired cosmogenic nuclides in Upernavik, northwest Greenland. Geological Society of America Bulletin 125, 1539-1553.
- Corbett, L.B., Bierman, P.R., Rood, D.H., 2016b. An approach for optimizing in situ cosmogenic ¹⁰Be sample preparation. Quaternary Geochronology 33, 24-34.
- Corbett, L.B., Bierman, P.R., Stone, B.D., Caffee, M.W., Larsen, P.L., 2017. Cosmogenic nuclide age estimate for Laurentide Ice Sheet recession from the terminal moraine, New Jersey, USA, and constraints on latest Pleistocene ice sheet history. Quaternary Research 87, 482-498.
- Davis, M.B., Spear, R.W., Shane, L.C., 1980. Holocene climate of New England. Quaternary Research 14, 240-250.

- Davis, P.T., 1999. Cirques of the Presidential Range, New Hampshire, and surrounding alpine areas in the northeastern United States. Geographie Physique et Quaternaire 53, 25-45.
- Davis, P.T., Bierman, P.R., Corbett, L.B., Finkel, R.C., 2015. Cosmogenic exposure age evidence for rapid Laurentide deglaciation of the Katahdin area, west-central Maine, USA, 16 to 15 ka. Quaternary Science Reviews 116, 95-105.
- Davis, P.T., Davis, R.B., 1980. Interpretation of minimum-limiting radiocarbon ages for deglaciation of Mt. Katahdin area, Maine. Geology 8, 396-400.
- Davis, P.T., Dethier, D.P., Nickmann, R., 1995. Deglaciation chronology and a late Quaternary pollen record from Woodford Bog, Bennington County, Vermont. Geological Society of America Abstracts with Programs 27, 38.
- Davis, P.T., Koester, A.J., Shakun, J.D., Bierman, P.R., Corbett, L.B., 2017. Testing the cosmogenic nuclide dipstick model for deglacaition of Mount Washington, New England Intercollegiate Geologic Conference Guidebook to Field Trips in Western Maine and Northern New Hampshire, pp. 247-272.
- Davis, R.B., Jacobson, G.L., 1985. Late glacial and early Holocene landscapes in northern New England and adjacent areas of Canada. Quaternary Research 23, 341-368.
- Dyke, A.S., 2004. An outline of North American deglaciation with emphasis on central and northern Canada. Quaternary Glaciations: Extent and Chronology 2, 373-424.
- Fabel, D., Harbor, J., 1999. The use of in-situ produced cosmogenic radionuclides in glaciology and glacial geomorphology. Annals of Glaciology 28, 103-110.
- Flint, R.F., 1951. Highland centers of former glacial outflow in northeastern North America.

 Bulletin of the Geological Society of America 62, 21-38.
- Gaudreau, D.C., Webb, T., 1985. Late-Quaternary pollen stratigraphy and isochrone maps for the northeastern United States, in: Bryant, V.M., Holloway, R.G. (Eds.), Pollen records of Late-Quaternary North American sediments. American Association of Stratigraphic Palynologists, pp. 247-280.
- Goehring, B., Wilson, J., Nichols, K., Accepted. A fully automated system for the extraction of in situ cosmogenic carbon-14 in the Tulane University Cosmogenic Nuclide Laboratory.

 Nuclear Instruments and Methods Section B: Beam Interactions with Materials and Atoms.
- Goehring, B.M., Brook, E.J., Linge, H., Raisbeck, G.M., Yiou, F., 2008. Beryllium-10 exposure ages of erratic boulders in southern Norway and implications for the history of the Fennoscandian Ice Sheet. Quaternary Science Reviews 27, 320-336.
- Goehring, B.M., Schaefer, J.M., Schluechter, C., Lifton, N.A., Finkel, R.C., Jull, A.J.T., Akçar, N., Alley, R.B., 2011. The Rhone Glacier was smaller than today for most of the Holocene. Geology 39, 679-682.
- Gosse, J.C., Evenson, E.B., Klein, J., Lawn, B., Middleton, R., 1995. Precise cosmogenic ¹⁰Be measurements in western North America: Support for a global Younger Dryas cooling event. Geology 23, 877-880.
- Gosse, J.C., Phillips, F.M., 2001. Terrestrial in situ cosmogenic nuclides: theory and application. Quaternary Science Reviews 20, 1475-1560.
- Granger, D.E., Muzikar, P.F., 2001. Dating sediment burial with in situ-produced cosmogenic nuclides: theory, techniques, and limitations. Earth and Planetary Science Letters 188, 269-281.

- Hall, B.L., Borns, H.W., Bromley, G.R.M., Lowell, T.V., 2017. Age of the Pineo Ridge System: Implications for behavior of the Laurentide Ice Sheet in eastern Maine, USA, during the last deglaciation. Quaternary Science Reviews 169, 344-356.
- Heyman, J., Applegate, P.J., Blomdin, R., Gribenski, N., Harbor, J.M., Stroeven, A.P., 2016.

 Boulder height exposure age relationships from a global glacial ¹⁰Be compilation.

 Quaternary Geochronology 34, 1-11.
- Hitchcock, E., Hager, A.D., Hitchcock, E.J., Hitchcock, C.H., 1861. Report on the Geology of Vermont: Descriptive, Theoretical, Economical, and Scenographical. Claremont Manufacturing Company, Claremont, NH.
- Hungerford, E., 1868. Evidences of glacial action on the Green Mountain summits. American Journal of Science and the Arts 45, 1-5.
- Johnson, J.S., Bentley, M.J., Smith, J.A., Finkel, R.C., Rood, D.H., Gohl, K., Balco, G., Larter, R.D., Schaefer, J.M., 2014. Rapid thinning of Pine Island Glacier in the early Holocene. Science 343, 99-1001.
- Jull, A.J.T., Scott, E.M., Bierman, P.R., 2015. The CRONUS-Earth inter-comparison for cosmogenic isotope analysis. Quaternary Geochronology 26, 3-10.
- Kleman, J., Borgstrom, I., 1994. Glacial land forms indicative of a partly frozen bed. Journal of Glaciology 40, 255-264.
- Koester, A.J., Shakun, J.D., Bierman, P.R., Davis, P.T., Corbett, L.B., Braun, D., Zimmerman, S.R., 2017. Rapid thinning of the Laurentide Ice Sheet in coastal Maine, USA, during late Heinrich Stadial 1. Quaternary Science Reviews 163, 180-192.
- Kohl, C.P., Nishiizumi, K., 1992. Chemical isolation of quartz for measurement of in-situproduced cosmogenic nuclides. Geochimica et Cosmochimica Acta 56, 3583-3587.
- Koteff, C., Pessl, F., 1981. Systematic ice retreat in New England. United States Government Printing Office, Washington DC.
- Lal, D., 1988. In situ-produced cosmogenic isotopes in terrestrial rocks. Annual Review of Earth and Planetary Sciences 16, 355-388.
- Lambeck, K., Rouby, H., Purcell, A., Sun, Y., Sambridge, M., 2014. Sea level and global ice volumes from the Last Glacial Maximum to the Holocene. Proceedings of the National Academy of Sciences of the United States of America 111, 15296-15303.
- Larsen, F.D., 1972. Glacial history of central Vermont, in: Doolan, B.D. (Ed.), New England Intercollegiate Geologic Conference Guidebook to Field Trips in Vermont, pp. 297-316.
- Larsen, F.D., 1987. History of lakes in the Dog River Valley central Vermont, in: Westerman, D.S. (Ed.), New England Intercollegiate Geologic Conference Guidebook to Field Trips in Vermont, pp. 213-237.
- Larsen, F.D., Wright, S.F., Springston, G.E., Dunn, R.K., 2003. Glacial, late-glacial, and postglacial history of central Vermont.
- Lifton, N., 2016. Implications of two Holocene time-dependent geomagnetic models for cosmogenic nuclide production rate scaling. Earth and Planetary Science Letters 433, 257-268.
- Lifton, N., Sato, T., Dunai, T.J., 2014. Scaling in situ cosmogenic nuclide production rates using analytical approximations to atmospheric cosmic-ray fluxes. Earth and Planetary Science Letters 386, 149-160.

- Lin, L., 1996. Environmental changes inferred from pollen analysis and ¹⁴C ages of pond sediments, Green Mountains, Vermont, Geology. University of Vermont, Burlington, VT, USA, p. 133.
- Liu, Z., Otto-Bliesner, B.L., He, F., Brady, E.C., Tomas, R., Clark, P.U., Carlson, A.E., Lynch-Stieglitz , J., Curry, W., Brook, E., Erickson, D., Jacob, R., Kutzbach, J., Cheng, J., 2009. Transient simulation of last deglaciation with a new mechanism for Bølling-Allerød warming. Science 325, 310-314.
- Long, A.J., 2009. Back to the future: Greenland's contribution to sea-level change. GSA Today 19 , 4-10.
- Loso, M.G., Schwartz, H.K., Wright, S.F., Bierman, P.R., 1998. Composition, morphology, and genesis of a moraine-like feature in the Miller Brook Valley, Vermont. Northeastern Geology and Environmental Sciences 20, 1-10.
- Margreth, A., Gosse, J.C., Dyke, A.S., 2016. Quantification of subaerial and episodic subglacial erosion rates on high latitude upland plateaus: Cumberland Peninsula, Baffin Island, Arctic Canada. Quaternary Science Reviews 133, 108-129.
- McDowell, L.L., Dole, R.M., Howard, M., Farrington, R.A., 1971. Palynology and radiocarbon chronology of Bugbee Wildflower Sanctuary and Natural Area, Caledonia Country, Vermont. Pollen and Spores XIII, 73-91.
- Miller, G.H., Briner, J.P., Lifton, N.A., Finkel, R.C., 2006. Limited ice-sheet erosion and complex exposure histories derived from in situ cosmogenic ¹⁰Be, ²⁶Al, and ¹⁴C on Baffin Island, Arctic Canada. Quaternary Geochronology 1, 74-85.
- Munroe, J.S., 2012. Lacustrine records of post-glacial environmental change from the Nulhegan Basin, Vermont, USA. Journal of Quaternary Science 27, 639-648.
- Munroe, J.S., Farrugia, G., Ryan, P.C., 2007. Parent material and chemical weathering in alpine soils on Mt. Mansfield, Vermont, USA. Catena 70, 39-48.
- Nishiizumi, K., Imamura, M., Caffee, M.W., Southon, J.R., Finkel, R.C., McAninch, J., 2007.

 Absolute calibration of ¹⁰Be AMS standards. Nuclear Instruments and Methods in Physics Research Section B: Beam Interactions with Materials and Atoms 258, 403-413.
- Nishiizumi, K., Kohl, C.P., Arnold, J.R., Dorn, R., Klein, I., Fink, D., Middleton, R., Lal, D., 1993. Role of in situ cosmogenic nuclides ¹⁰Be and ²⁶Al in the study of diverse geomorphic processes. Earth Surface Processes and Landforms 18, 407-425.
- Nishiizumi, K., Winterer, E.L., Kohl, C.P., Klein, J., Middleton, R., Lal, D., Arnold, J.R., 1989.

 Cosmic ray production rates of ¹⁰Be and ²⁶Al in quartz from glacially polished rocks.

 Journal of Geophysical Research 94, 17907.
- Noren, A.J., 2002. A 13,000-year regional record of Holocene storms in the northeastern United States, Geology. University of Vermont, Burlington, VT, p. 179.
- Noren, A.J., Bierman, P.R., Steig, E.J., Lini, A., Southon, J., 2002. Millennial-scale storminess variability in the northeastern United States during the Holocene epoch. Nature 419, 821-824.
- Parent, M., Dube-Loubert, H., 2017. Middle and Late Wisconsinan events and stratigraphy in southern Quebec- A new pre-LGM marine incursion. McGill University.
- Parris, A.S., 2003. Holocene paleohydrology in the northeastern United States: a high resolution record of storms and floods, Geology. University of Vermont, Burlington, VT, p. 141.

- Parris, A.S., Bierman, P.R., Noren, A.J., Prins, M.A., Lini, A., 2010. Holocene paleostorms identified by particle size signatures in lake sediments from the northeastern United States. Journal of Paleolimnology 43, 29-49.
- Phillips, F.M., Zreda, M.G., Smith, S.S., Elmore, D., Kubik, P.W., Sharma, P., 1990. Cosmogenic chlorine-36 chronology for glacial deposits at Bloody Canyon, eastern Sierra Nevada. Science 248, 1529-1532.
- Ratcliffe, N.M., Stanley, R.S., Gale, M.H., Thompson, P.J., Walsh, G.J., 2011. Bedrock geologic map of Vermont, in: Estabrook, J.R. (Ed.), US Geological Survey Scientific Investigations Map 3184 1:100,000. US Geological Survey.
- Rayburn, J.A., Franzi, D.A., Knuepfer, P.L.K., 2007. Evidence from the Lake Champlain Valley for a later onset of the Champlain Sea and implications for late glacial meltwater routing to the North Atlantic. Palaeogeography, Palaeoclimatology, Palaeoecology 246, 62-74.
- Rayburn, J.A., Knuepfer, P.L.K., Franzi, D.A., 2005. A series of large, Late Wisconsinan meltwater floods through the Champlain and Hudson Valleys, New York State, USA. Quaternary Science Reviews 24, 2410-2419.
- Reimer, P., Bard, E., Bayliss, A., Beck, J.W., Blackwell, P.G., Ramsey, C.B., Buck, C.E., Cheng, H., Edwards, R.L., Friedrich, M., Grootes, P.M., Guilderson, T.P., Haflidason, H., Hajdas, I., Hatte, C., Heaton, T.J., Hoffman, D.L., Hogg, A.G., Hughen, K.A., Kaiser, K.F., Kromer, B., Manning, S.W., Niu, M., Reimer, R.W., Richards, D.A., Scott, E.M., Southon, J.R., Staff, R. A., Turney, C.S.M., van der Plicht, J., 2013. IntCal13 and Marine13 radiocarbon age calibration curves 0–50,000 years cal BP. Radiocarbon 55, 1869-1887.
- Richard, P.J.H., Occhietti, S., 2005. ¹⁴C chronology for ice retreat and inception of the Champlain Sea in the St Lawrence Lowlands, Canada. Quaternary Research 63, 353-358.
- Ridge, J.C., 2004. The Quaternary glaciation of western New England with correlations to surrounding areas, Developments in Quaternary Sciences. Elsevier, pp. 169-199.
- Ridge, J.C., Balco, G., Bayless, R.L., Beck, C.C., Carter, L.B., Cean, J.L., Voytek, E.B., Wei, J.H., 2012
 . The new North American varve chronology: A precise record of southeastern
 Laurentide Ice Sheet deglaciation and climate 18.2-12.5 kyr BP, and correlations with
 Greenland Ice Core records. American Journal of Science 312, 685-722.
- Ridge, J.C., Besonen, M.R., Brochu, M., Brown, S.L., Callahan, J.W., Cook, G.J., Nicholson, R.S., Toll, N.J., 1999. Varve, paleomagnetic, and ¹⁴C chronologies for Late Pleistocene events in New Hampshire and Vermont (U.S.A.). Geographie Physique et Quaternaire 53, 79-106.
- Rogers, J.N., Fowler, B.K., McCoy, W.D., Davis, P.T., 2009. Post-glacial mass wasting in Franconia Notch, White Mountains, New Hampshire, in: Westerman, D.S., Lathrop, A.S. (Eds.), New England Intercollegiate Geologic Conference Guidebook to Field Trips in the Northeast Kingdom of Vermont and Adjacent Regions, Lyndonville, Vermont, pp. 199-223.
- Schildgen, T.F., Phillips, W.M., Purves, R.S., 2005. Simulation of snow shielding corrections for cosmogenic nuclide surface exposure studies. Geomorphology 64, 67-85.
- Shotton, F.W., 1972. An example of hard water error in radiocarbon dating of vegetable matter. Nature 240, 460-461.
- Siddall, M., Rohling, E.J., Arz, H.W., 2008. Convincing evidence for rapid ice sheet growth during the last glacial period. PAGES News 16, 15-16.

- Spear, R.W., 1989. Late-Quaternary History of High-Elevation Vegetation in the White Mountains of New Hampshire. Ecological Monographs 59, 125-151.
- Spear, R.W., Davis, M.B., Shane, L.C.K., 1994. Late Quaternary History of Low- and Mid-Elevation Vegetation in the White Mountains of New Hampshire. Ecological Monographs 64, 85-109.
- Sperling, J.A., Wehrle, M.E., Newman, W.S., 1989. Mountain glaciation at Ritterbush Pond and Miller Brook, Northern Vermont, reexamined. Northeastern Geology 11, 106-111.
- Stone, J.O., Balco, G.A., Sugden, D.E., Caffee, M.W., Sass III, L.C., Cowdery, S.G., Siddoway, C., 2003. Holocene deglaciation of Marie Byrd Land, West Antarctica. Science 299, 99-102.
- Stone, J.O., Ballantyne, C.K., Fifield, L.K., 1998. Exposure dating and validation of periglacial weathering limits, northwest Scotland. Geology 26, 587-590.
- Stuiver, M., Reimer, P.J., Reimer, R., 2015. CALIB Radiocarbon Calibration 7.1. calib.qub.ac. uk/calib/.
- Sugden, D.E., 1977. Reconstruction of the morphology, dynamics, and thermal characteristics of the Laurentide Ice Sheet at its maximum. Arctic and Alpine Research 9, 21-47.
- Sugden, D.E., 1978. Glacial erosion by the Laurentide ice sheet. Journal of Glaciology 20, 367-391.
- Sugden, D.E., Balco, G., Cowdery, S.G., Stone, J.O., Sass III, L.C., 2005. Selective glacial erosion and weathering zones in the coastal mountains of Marie Byrd Land, Antarctica. Geomorphology 67, 317-334.
- Sugden, D.E., Watts, S.H., 1977. Tors, felsenmeer, and glaciation in northern Cumberland Peninsula, Baffin Island. Canadian Journal of Earth Sciences 14, 2817-2823.
- Thompson, W.B., Crossen, K.J., Andersen, B.G., 1989. Glaciomarine deltas of Maine and their relation to Late Pleistocene-Holocene Crustal movements, in: Andersen, W.A., Borns, H. W. (Eds.), Neotectonics of Maine; Studies in Seismicity, Crustal Warping, and Sea-level Change. Maine Geological Survey, Augusta, Maine, pp. 43-67.
- Thompson, W.B., Dorion, C.C., Ridge, J.C., Balco, G., Fowler, B.K., Svendsen, K.M., 2017.

 Deglaciation and late-glacial climate change in the White Mountains, New Hampshire, U. S.A. Quaternary Research 87, 96-120.
- Thompson, W.B., Fowler, B.K., Flanagan, S.M., Dorion, C.C., 1996. Recession of the Late Wisconsinan ice sheet from the northwestern White Mountains, N.H., in: Van Baalen, M. R. (Ed.), New England Intercollegiate Geologic Conference Guidebook to Field Trips in Northern New Hampshire and Adjacent Regions of Maine and Vermont. Harvard University, Cambridge, Massachusetts, pp. 203-234.
- Wagner, W.P., 1970. Pleistocene mountain glaciation, northern Vermont. Geological Society of America Bulletin 81, 2465-2470.
- Waitt, R.B., Davis, P.T., 1988. No evidence for post-icesheet cirque glaciation in New England.

 American Journal of Science 288, 495-533.
- Whitehead, D.R., Jackson, S.T., 1990. The regional vegetation history of the High Peaks, Adirondack Mountains, New York. New York State Museum Bulletin 478, 1-36.
- Winsor, K., Carlson, A.E., Caffee, M.W., Rood, D.H., 2015. Rapid last-deglacial thinning and retreat of the marine-terminating southwestern Greenland ice sheet. Earth and Planetary Science Letters 426, 1-12.

- Wright, S.F., 2001. Surficial geology of the Jeffersonville quadrangle, Vermont, Vermont Geological Survey Open-File Report VG01-2. Vermont Geological Survey, Montpelier, VT.
- Wright, S.F., 2015. Late Wisconsinan ice sheet flow across northern and central Vermont, USA. Quaternary Science Reviews 129, 216-228.
- Wright, S.F., 2017. Ice streaming in the southern Champlain and northern Hudson river valleys, Vermont and New York. Geological Society of America Abstracts with Programs 49.
- Wright, S.F., 2018. Surficial geology and hydrogeology of the Bolton Mountain Quadrangle, Vermont Geological Survey Open File report VG2018-4. Vermont Geological Survey, Montpelier, VT.
- Wright, S.F., Whalen, T.N., Zehfuss, P.H., Bierman, P.R., 1997. Late Pleistocene-Holocene history: Huntington River and Miller Brook valleys, northern Vermont, in: Grover, T.W., Mango, H.N., Hasenohr, E.J. (Eds.), New England Intercollegiate Geologic Conference Guidebook to Field Trips in Vermont and adjacent New Hampshire and New York, pp. C4: 1-30.
- Zimmerman, S.G., Evenson, E.B., Gosse, J.C., Erskine, C.P., 1994. Extensive boulder erosion resulting from a range fire on the type-Pinedale moraines, Fremont Lake, Wyoming. Quaternary Research 42, 255-265.